

# UCLA

## UCLA Previously Published Works

### Title

Evidence for even parity unconventional superconductivity in Sr<sub>2</sub>RuO<sub>4</sub>

### Permalink

<https://escholarship.org/uc/item/4bm235f6>

### Journal

Proceedings of the National Academy of Sciences of the United States of America, 118(25)

### ISSN

0027-8424

### Authors

Chronister, Aaron  
Pustogow, Andrej  
Kikugawa, Naoki  
[et al.](#)

### Publication Date

2021-06-22

### DOI

10.1073/pnas.2025313118

Peer reviewed

# Evidence for even parity unconventional superconductivity in Sr<sub>2</sub>RuO<sub>4</sub>

Aaron Chronister<sup>a,1,2</sup>, Andrej Pustogow<sup>a,1,2,3</sup> , Naoki Kikugawa<sup>b</sup>, Dmitry A. Sokolov<sup>c</sup>, Fabian Jerzembeck<sup>c</sup> , Clifford W. Hicks<sup>c,d</sup> , Andrew P. Mackenzie<sup>c,e</sup> , Eric D. Bauer<sup>f</sup>, and Stuart E. Brown<sup>a,2</sup> 

<sup>a</sup>Department of Physics & Astronomy, University of California, Los Angeles, CA 90095; <sup>b</sup>Cryogenic Center for Liquid Hydrogen and Materials Science, National Institute for Materials Science, Tsukuba 305-0003, Japan; <sup>c</sup>Physics of Quantum Materials Department, Max Planck Institute for Chemical Physics of Solids, Dresden 01187, Germany; <sup>d</sup>School of Physics and Astronomy, University of Birmingham, Birmingham B15 2TT, United Kingdom; <sup>e</sup>Scottish Universities Physics Alliance, School of Physics and Astronomy, University of St Andrews, St Andrews KY16 9SS, United Kingdom; and <sup>f</sup>Materials Physics and Applications, Los Alamos National Laboratory, Los Alamos, NM 87545

Edited by Angel Rubio, Max Planck Institute for the Structure and Dynamics of Matter, Hamburg, Germany, and approved May 16, 2021 (received for review December 10, 2020)

**Unambiguous identification of the superconducting order parameter symmetry in Sr<sub>2</sub>RuO<sub>4</sub> has remained elusive for more than a quarter century. While a chiral *p*-wave ground state analogue to superfluid <sup>3</sup>He-A was ruled out only very recently, other proposed triplet-pairing scenarios are still viable. Establishing the condensate magnetic susceptibility reveals a sharp distinction between even-parity (singlet) and odd-parity (triplet) pairing since the superconducting condensate is magnetically polarizable only in the latter case. Here field-dependent <sup>17</sup>O Knight shift measurements, being sensitive to the spin polarization, are compared to previously reported specific heat measurements for the purpose of distinguishing the condensate contribution from that due to quasiparticles. We conclude that the shift results can be accounted for entirely by the expected field-induced quasiparticle response. An upper bound for the condensate magnetic response of < 10% of the normal state susceptibility is sufficient to exclude all purely odd-parity candidates.**

unconventional superconductivity | triplet pairing | Knight shift | nuclear magnetic resonance | order parameter

Unraveling the secrets of the superconducting state in Sr<sub>2</sub>RuO<sub>4</sub> (1–3) has been a priority for unconventional superconductivity research since its discovery in 1994, by Maeno et al. (4). Among several reasons for broad interest in Sr<sub>2</sub>RuO<sub>4</sub> was the particularly notable suggestion of a *p*-wave triplet pairing state (5). One of the symmetry-allowed triplet states is the chiral state  $\mathbf{z}(p_x \pm ip_y)$ , which breaks time reversal symmetry and therefore requires two components. Soon after, the combination of results from NMR Knight shift (6) and  $\mu^+$ SR (7) measurements lent support to the chiral *p*-wave description. Further evidence was inferred from the observed onset of a nonzero Kerr rotation at  $T_c$  (8). Unresolved issues remained, however. For example, thermal conductivity (9) and specific heat (10) experiments were both interpreted as evidence for a nodal gap structure (3). Furthermore, the field-driven first-order phase transition observed at low temperatures (11, 12) is a natural consequence of the Zeeman coupling to quasiparticles (1), but this mechanism is inoperative for any fully gapped state. In a step toward clarification, recent <sup>17</sup>O NMR measurements exclude candidate *p*-wave states with **k**-independent **d**-vector aligned parallel to the *c* axis (13, 14). Left open is the possibility for an odd-parity triplet-pairing state with an in-plane **d**, as explicitly discussed in recent theoretical works (15, 16).

With these developments in mind, we recall other distinctive properties of superconductivity in Sr<sub>2</sub>RuO<sub>4</sub>. Among unconventional superconductors, Sr<sub>2</sub>RuO<sub>4</sub> is not just stoichiometric but possibly also the cleanest (1). Unlike the cuprates (17) and Fe-based superconductors, the superconductivity emerges from a well-understood Fermi liquid normal state (18), and for which the fermiology is precisely characterized (19, 20). Thus, Sr<sub>2</sub>RuO<sub>4</sub>

constitutes an ideal platform for achieving a level of understanding for an unconventional superconductor rivaling what is routinely expected for conventional superconductors. In general, identifying the order parameter symmetry is an essential step toward that goal. Moreover, there is a broader motivation to make connections from a system so well characterized, to other unresolved questions in unconventional superconductivity. As described above, Sr<sub>2</sub>RuO<sub>4</sub> was reasonably proposed as analogous to <sup>3</sup>He, for which ferromagnetic (FM) fluctuations are key to the superfluid triplet pairing. Indeed, the presence of FM correlations was inferred early on (4, 5). In an alternative proposal, the system is a more weakly coupled analog of the cuprate and Fe-based superconductors, in which antiferromagnetic fluctuations most naturally mediate singlet pairing (21). Thus, associating the superconducting state with AF fluctuations would more directly relate the physics of Sr<sub>2</sub>RuO<sub>4</sub> to the much broader class of unconventional superconductors.

The temperature and field dependences of the NMR Knight shifts  $K_s(T < T_c, \mathbf{B})$  are recognized as a crucial probe of the order-parameter symmetry. In the normal state,  $K_s \sim \chi_n$ , with

## Significance

**Sr<sub>2</sub>RuO<sub>4</sub> is distinctive among unconventional superconductors, in that in addition to exhibiting evidence for strong correlations, it is stoichiometric and extremely clean. As a result, its electronic structure is unusually well characterized, rendering it an ideal platform for developing a deep understanding of the mechanism behind the emergence of the superconducting state from a Fermi liquid. Toward that end, an unambiguous determination of the pairing symmetry is an essential step. For more than 2 decades, the preponderance of evidence pointed to a triplet spin pairing state and only recently has this interpretation been challenged. By field-dependent NMR Knight shift measurements, we eliminate from further consideration all candidate purely odd-parity triplet pairing states.**

Author contributions: A.C., A.P., and S.E.B. designed research; A.C. and A.P. performed research; A.C., A.P., and S.E.B. analyzed data; N.K., D.A.S., F.J., and E.D.B. contributed new reagents/analytic tools; N.K. monitored sample growth; D.A.S., F.J., C.W.H., and A.P.M. contributed to sample characterization; E.D.B. contributed to sample alignment, cutting, and oxygenation; and A.C., A.P., C.W.H., A.P.M., and S.E.B. wrote the paper.

The authors declare no competing interest.

This article is a PNAS Direct Submission.

Published under the [PNAS license](#).

<sup>1</sup>A.C. and A.P. contributed equally to this work.

<sup>2</sup>To whom correspondence may be addressed. Email: aaronchronister@ucla.edu, pustogow@ifp.tuwien.ac.at, or brown@physics.ucla.edu.

<sup>3</sup>Present address: Institute of Solid State Physics, TU Wien, 1040 Vienna, Austria.

This article contains supporting information online at <https://www.pnas.org/lookup/suppl/doi:10.1073/pnas.2025313118/-/DCSupplemental>.

Published June 14, 2021.

$\chi_n$  the susceptibility. In the superconducting phase, a nonzero susceptibility  $\chi_{sc}$  associated with condensate polarization is expected generally for triplet-paired,  $p$ -wave states. The response ranges from vanishingly small to that of the normal state,  $\chi_n$ , with the limiting cases corresponding to  $\mathbf{d} \parallel \mathbf{B}$ ,  $\mathbf{d} \perp \mathbf{B}$ , respectively. Hence, the observed reduction of the Knight shift for an applied in-plane field excludes the chiral state (13), for which  $\mathbf{d} \parallel \mathbf{c}$ . Crucially, states characterized by  $\mathbf{d} \perp \mathbf{c}$  are not eliminated by the prior work. Among such states allowed by the crystal symmetry is the so-called “helical” state,  $\mathbf{d} = p_x \mathbf{x} + p_y \mathbf{y}$ , for which  $\chi_{sc}/\chi_n = 1/2$  [in the absence of Fermi-liquid corrections (13, 14)].

The most direct way to test for symmetry-allowed states with  $\mathbf{d} \perp \mathbf{c}$  is to perform measurements with  $\mathbf{B} \parallel \mathbf{c}$ , since for this orientation the response of the helical state is  $\chi_{sc} = \chi_n$ . However, the relevant upper critical field  $B_{c2,[001]} < 100$  mT is very small\* making such experiments particularly challenging because signal strength and spectral resolution are reduced for very weak applied fields. Here we take another approach, discussed previously in refs. 14, 23: the field orientation is fixed in-plane, and the  $^{17}\text{O}$  shifts  $K_s$  are evaluated at low temperature (25 mK) while varying  $B$  as much as experimentally feasible. Quasiparticle creation is controlled by the field strength and also contributes to the magnetic response. At issue is the fractional magnetic response arising from quasiparticles, which must be separated from the condensate contribution. The relative contributions are determined by way of comparing to previously reported specific heat results  $C_e(B)/T$  (24), which is sensitive to field-induced quasiparticles only. We estimate that the upper bound for the condensate portion is  $\chi_{sc}/\chi_n < 10\%^\dagger$ , a value that contradicts the expectation for any of the proposed purely odd-parity order parameters relevant to  $\text{Sr}_2\text{RuO}_4$ .

## Results

**Pulse-Heating Control by Low-Power NMR Experiments.** The recent studies (13, 14) identified radio frequency (RF) heating by the NMR pulses as a possible impediment to accurate measurements in the superconducting state. The issue is illustrated in the results of Fig. 1. So as to enhance sensitivity to this potential artifact, we examined the transients with the field set to 1.38 T, a value very close to but smaller than  $B_{c2}$ . Clear evidence for warming by the RF pulsing is inferred from a transient response corresponding to that of the normal state (instead of the sought-after superconducting state). Shown in Fig. 1 B and C are  $^{17}\text{O}$  spectra corresponding to central transitions for the three oxygen sites,  $\text{O}(1_{\parallel}, 2, 1_{\perp})$ , at applied magnetic fields slightly above and below  $B_{c2}$ . With  $B = 1.5 \text{ T} > B_{c2}$ , the line shape remains unaffected by changing the pulse energy, and a normal state spectrum is also produced for  $B = 1.38 \text{ T} < B_{c2}$  when using a pulse energy  $E_p = 130 \text{ nJ}$ . Decreasing  $E_p$  to 40 nJ leads to a response where a new spectral line appears for each site, indicating the coexistence of normal and superconducting phases. This dataset is particularly useful since the macroscopic phase segregation provides a quantitative measure of the magnetization jump  $\Delta M$  at the discontinuous (first-order) transition (11, 12). Note that these data are recorded following a single-pulse excitation. That is, the transient NMR response corresponds to a free induction decay (FID). All shift results of the present work were obtained from FID measurements carried out with RF pulse energies sufficiently small to avoid heating, as illustrated in Fig. 1D.

**Field-Dependent Knight Shifts in the Superconducting State.** Having established a threshold for heating effects, we now inspect the

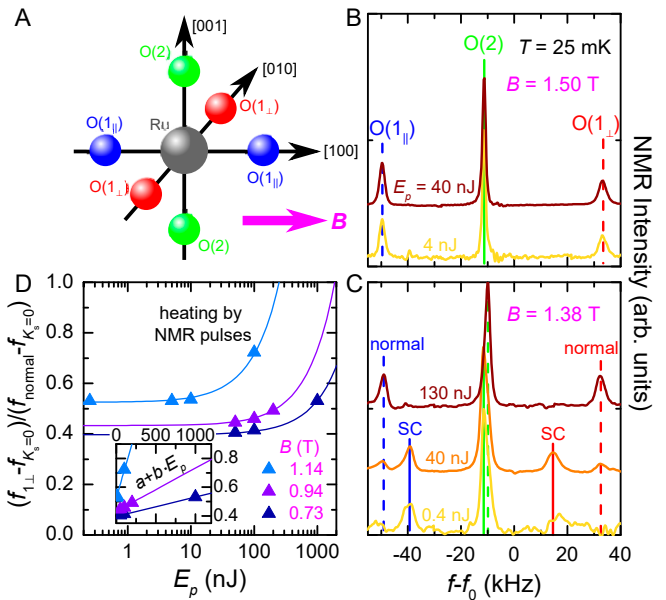


**Fig. 1.** (A)  $\text{Sr}_2\text{RuO}_4$  involves three distinct oxygen sites for field direction  $\mathbf{B} \parallel [100]$ . (B) The three associated  $^{17}\text{O}$  NMR central transitions [ $\text{O}(1_{\parallel})$ ,  $\text{O}(2)$ , and  $\text{O}(1_{\perp})$ , from left to right] are independent of pulse energy  $E_p$  at  $1.50 \text{ T} > B_{c2} \approx 1.45 \text{ T}$ . (C) Also at  $B = 1.38 \text{ T} \lesssim B_{c2}$  the normal-state spectrum is observed for  $E_p \geq 10^{-7} \text{ J}$ . Reducing to  $E_p = 40 \text{ nJ}$  leads to doubled spectral features, most pronounced for  $\text{O}(1_{\parallel, \perp})$ , which we assign to coexisting normal (dashed vertical lines) and superconducting (solid) contributions around the first-order transition. Further reduction of  $E_p$  reveals the pure superconducting-state spectrum. (D)  $\text{O}(1_{\perp})$  frequencies normalized to normal-state ( $f_{\text{normal}}$ ) and zero-shift ( $f_{K_s=0}$ ; Fig. 2) positions at  $B < B_{c2}$  for variable  $E_p$ . Linear fits (solid lines; Inset) indicate that heating is less problematic at lower field due to larger  $T_c(B)$ . Knight shifts  $K_s$  were determined using the frequency values leveling off at  $E_p \rightarrow 0$ .

spectra recorded at variable field strength. In Fig. 2, we show the NMR intensity as a function of  $f - f_0$ , where  $f_0 \equiv \frac{1}{2} \gamma B$ . The central transitions ( $-1/2 \leftrightarrow 1/2$ ) for the  $\text{O}(1_{\parallel}, 2, 1_{\perp})$  sites (left to right in the spectrum) exhibit pronounced variations with changing  $B$ . The shifts of the planar sites  $\text{O}(1_{\parallel})$  and  $\text{O}(1_{\perp})$  have opposite sign; this is a consequence of the applied field direction relative to the local environment.  $\text{O}(2)$  is the apical site (Fig. 1A). The dotted curves include only the quadrupolar and orbital contributions for each site, while omitting the Knight shift contribution; more information on these corrections appears below.<sup>†</sup> Crucially, simultaneous scrutiny of the field-dependent quadrupolar effects at both in-plane O sites leads to a quantitative upper bound on the condensate contribution. Open symbols line up with these spectral baselines at each field at which data were recorded. Also shown, using the dashed lines and closed symbols, are transition frequencies at each field, generated using the known normal state NMR parameters.<sup>†</sup> Then, the frequency differences between closed and open symbols are proportional to the hyperfine fields and constitute the product of (normal-state) Knight shifts with applied field,  $K_{s,\text{normal}} \frac{1}{2} \gamma B$ , for  $\text{O}(1_{\parallel})$ ,  $\text{O}(2)$ , and  $\text{O}(1_{\perp})$ . When decreasing the field  $B < B_{c2}$ , the NMR lines in Fig. 2 are displaced from the normal-state positions, toward the frequency corresponding to  $K_s = 0$ , due to the drop of  $K_s$  in the superconducting state. Below, we compare and contrast the measured shifts  $K_s$  with results of field-dependent specific heat experiments, which are sensitive to the field-induced quasiparticles.

The parameters needed for the quadrupolar corrections were determined previously (6, 25, 26) and confirmed here in field-dependent measurements.<sup>†</sup> In particular, we determined the field orientation as deviating  $\approx 3.0^\circ \pm 0.4^\circ$  from the

\* a-axis stress increases  $B_{c2}$  significantly by this measure (22).

<sup>†</sup> See SI Appendix for details on the discontinuous transition at  $B_{c2}$ , the different contributions to  $^{17}\text{O}$  NMR shifts, and sample alignment with respect to the external magnetic field.

[100] direction and otherwise aligned orthogonal to the  $c$  axis,  $\theta = 90^\circ \pm 0.2^\circ$ . Due to several factors, including reduced signal strength and resolution, as well as the strong increase of the  $O(1_{\parallel})$  quadrupolar component at low fields, we limited the measurements to  $B \geq 0.24$  T. In addition to the well-known quadrupolar effects, one has to include purely orbital contributions. These were evaluated in ref. 6, yielding  $K_o = +0.18\%$  for the  $O(1_{\parallel})$  site and a value indistinguishable from zero for  $O(1_{\perp})$  and  $O(2)$ .<sup>†</sup>

The shifts  $K_{1_{\parallel},2,1_{\perp}}$  are plotted as a function of  $B$  in Fig. 3. Results are shown in Fig. 3A as total shift,  $K = K_s + K_o$ . In the normal state,  $K_{1_{\parallel}} < 0$ , while  $K_{2,1_{\perp}} > 0$ ; each exhibits a reduction in the superconducting state.  $B_{c2}$  is marked by the discontinuous change of each of the three sites, accompanied by a coexistence regime (cf. Fig. 1 B and C). Consistent with expectations ( $B \gg B_{c1}$ ) (27), the results indicate that diamagnetic shielding is a small effect. Otherwise, the discontinuous drop  $\Delta M$  (Figs. 1 and 2) would be similar for all three sites. Instead, only the hyperfine field, which is much greater for the planar sites than it is for the apical site, and opposite in sign for  $O(1_{\parallel})$  relative to  $O(2)$  and  $O(1_{\perp})$ , decreases on entering the superconducting state.

**Comparison to Specific Heat: Condensate Polarization vs. Field-Induced Quasiparticles.** The main results of this work are displayed in Fig. 3B, where the Knight shifts are compared to previous heat capacity results (24),  $C_e(B)/T$  ( $C_e$  is the electronic contribution), both normalized to the normal state. As shown, the field-induced trends are similar and particularly relevant to the open question of order-parameter symmetry. Simply put, at nonzero field, an NMR shift can originate from quasiparticles and, in the case of triplet pairing, also from the condensate. In contrast, the specific heat is sensitive only to the quasiparticle

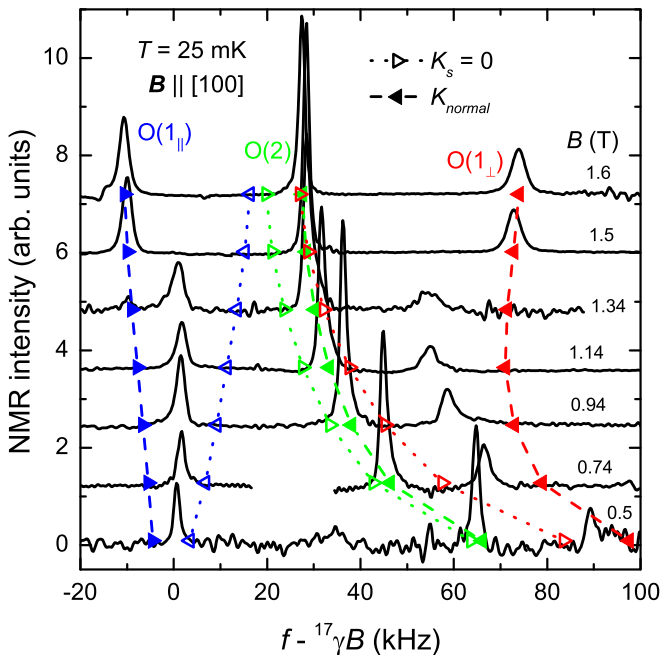


Fig. 2. Spectra for central  $^{17}\text{O}$  NMR transitions at different field strengths, for  $O(1_{\parallel})$ ,  $O(2)$ , and  $O(1_{\perp})$  sites, from left to right, plotted as intensity vs.  $f - ^{17}\gamma B$ . The dotted curves running vertically through the spectra follow the expected field dependence after taking into account quadrupolar and orbital couplings; the dashed curves also include the normal-state hyperfine fields. We provide details of quadrupolar and orbital contributions to the transition frequencies, as well as an analysis of the sample orientation relative to  $\mathbf{B}$ .<sup>†</sup>

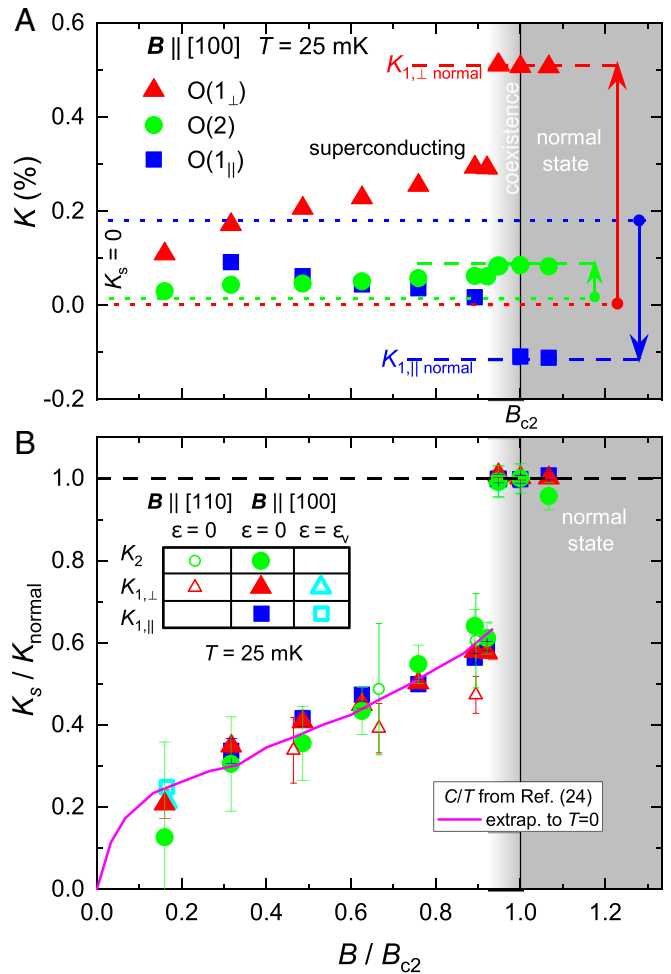


Fig. 3. (A) NMR shifts  $K = K_s + K_o$  determined from the spectra in Fig. 2. While the shifts are positive and the assigned  $K_o \approx 0.0\%$  for  $O(2)$  and  $O(1_{\perp})$ , the  $O(1_{\parallel})$  line occurs at a positive value  $K_o = 0.18\%$  at  $B = 0$  and  $K_{1_{\parallel}} < 0$  (6, 25). (B) The field-dependent drop of NMR Knight shift determined in the present work at  $T = 25$  mK is compared to specific heat  $C/T$  (24) extrapolated to  $T = 0^{\ddagger}$ , all normalized to the normal state value. The values of  $K_s$  coincide with the zero-temperature extrapolations of  $C/T$ , providing compelling evidence that this is the contribution of unpaired quasiparticles in the superconducting state. Measurements along  $[110]$  (small open symbols) reveal a similar jump at the transition, and also uniaxial strain results (open cyan symbols,  $\mathbf{B} \parallel [100]$ ,  $\epsilon_{aa} = \epsilon_v$ ) from ref. 13 coincide at low  $B/B_{c2}$ .

response with no contribution from the condensate. Note that in a fully gapped superconductor, gapless excitations are created in vortex cores, where the order parameter is suppressed. Whereas, in the case of a nodal state, the quasiparticle perturbations arising from both Zeeman and orbital coupling lead to additional contributions to the density of states (DOS) at  $E_F$ . [The latter is widely referred to as the Volovik effect (28).]

As can be seen by inspection of Fig. 3B, we observe no systematic difference between the  $T \rightarrow 0$  extrapolation of the heat capacity data of ref. 24 and the spin susceptibility deduced from our measurements. Taking into account systematic uncertainties we estimate an upper limit for the condensate response of

<sup>†</sup>We also note that recent specific heat measurements (10, 20) differ from those of ref. 24 by finding a larger residual electronic specific heat at low temperatures. While sample quality is the most obvious source of such a discrepancy, it merits further experimental attention. However, since those results indicate a larger quasiparticle contribution (than that of ref. 24), the central conclusion of the present work is not invalidated: we find no evidence for a condensate contribution to the spin susceptibility.

< 10% of that of the normal state, for fields applied both along [100] and [110].<sup>†</sup> Similar  $K_{1||,\perp}$  are found at  $B/B_{c2} = 0.17$  under strained conditions (13). These observations place such strong constraints on the magnetic polarizability of the condensate that we believe they rule out any pure  $p$ -wave order parameter for the superconducting state of  $\text{Sr}_2\text{RuO}_4$ , as we now discuss.

The  $p$ -wave order parameters most commonly discussed in the context of  $\text{Sr}_2\text{RuO}_4$  are the so-called chiral  $[\hat{z}(p_x \pm ip_y)]$  and helical  $(p_x\hat{x} + p_y\hat{y})$  states. Assuming that the unit vectors encoding spin directions are pinned to the lattice, they are predicted in the simplest models to result in condensate polarizabilities of 100% (chiral) and 50% (helical) of the normal state value. The chiral state was ruled out by our previous work (13), but the helical state and certain others were not. The data presented in Fig. 3 allow us to go much further; it is unclear how to reconcile an upper bound of 10% of the normal state susceptibility with any  $p$ -wave state. While Fermi liquid corrections may reduce the condensate response to  $\sim 30\%$  of the normal state value (14), this still far exceeds our observations. Spin-orbit coupling (SOC) effects tend to weaken the distinction between spin-singlet and spin-triplet states (29), in that a nonzero magnetic response survives in the limit  $T, B \rightarrow 0$  (16). Thus, we conclude that SOC effects are not significantly impacting our results, an outcome we tentatively attribute to the dominant normal state DOS (and magnetic response) arising from those states at  $E_F$  proximate to a van Hove singularity, where the SOC is relatively weak (26). One could also postulate extreme situations such as a momentum-independent  $\mathbf{d}$  aligned along either [100] or [110] or an unpinned  $\mathbf{d}$  free to rotate in response to the applied field. None result in a spin susceptibility suppression compatible with our results; a few remaining possibilities are eliminated by our use of both [100] and [110] fields in the current experiments. We therefore assert that our measurements have ruled out any  $p$ -wave order parameter candidate for the superconducting state of  $\text{Sr}_2\text{RuO}_4$ .

## Summary and Outlook

Given this input, we close with an evaluation of the current understanding of superconductivity in  $\text{Sr}_2\text{RuO}_4$ . In isolation, our NMR findings are consistent with even-parity states (30), such as  $d_{x^2-y^2}$  ( $B_{1g}$ ),  $d_{xy}$  ( $B_{2g}$ ) or  $\{d_{xz}; d_{yz}\}$  ( $E_{1g}$ ), or  $g_{xy(x^2-y^2)}$  ( $A_{2g}$ ). Indeed, scanning tunneling microscopy measurements are interpreted as most consistent with the  $B_{1g}$  state (31), similar to thermal transport experiments (9). Further emphasizing the constraints imposed by the present work, the viability of proposed even-parity states based on interorbital pairing (32–34), and that of a mixed-parity order parameter of the form  $d \pm ip$  (35) necessarily depends on a sufficiently small condensate response to in-plane fields.

In considering other recent experimental developments, we would like to note in particular reports of a discontinuity in the shear elastic constant  $c_{66}$  (corresponding to  $B_{2g}$  deformations) (36, 37) but not in  $(c_{11} - c_{12})/2$  ( $B_{1g}$ ) (36). This is the expected outcome for a coupling of nearly degenerate even-parity states such as  $\{d_{x^2-y^2}; g_{xy(x^2-y^2)}\}$  (21, 38) or  $\{s'; d_{xy}\}$  (39) but not for the degenerate combination  $\{d_{xz}; d_{yz}\}$ , for which a discontinuity in  $(c_{11} - c_{12})/2$  is also expected. On the other hand,  $\mu^+$ SR measurements have confirmed the early results and observed transition splitting between the TRSB signature and the onset of SC under uniaxial pressure (40). It will be intriguing to see how the quest to finalize identification of the order parameter of  $\text{Sr}_2\text{RuO}_4$  develops.

## Materials and Methods

**Sample Preparation.** As in previous NMR studies on  $\text{Sr}_2\text{RuO}_4$  (6), the labeled  $^{17}\text{O}$  [ $^{17}I = 5/2$ ,  $^{17}\gamma = -5.772$  MHz/T (41)] is introduced by high-temperature annealing (6), here in 90%  $^{17}\text{O}_2$  atmosphere at 1,050 °C. Single-crystal dimensions were (3.5 mm  $\times$  1 mm  $\times$  0.2 mm), with the shortest dimension corresponding to the out-of-plane [001] direction and the longest dimension parallel to [100] (Fig. 1A).

**NMR Experiments.** To facilitate access to relatively low frequencies covering several octaves, we adopted a top tuning/matching configuration. The NMR coil containing the crystal under study was mounted on a single-axis piezorotator inside the mixing chamber of a bottom-loading dilution refrigerator. Sample alignment enabled in-plane orientation to within  $\pm 0.2^\circ$ , based on RF susceptibility measurements sensitive to  $B_{c2}$ , described in ref. 13 and discussed in *SI Appendix*.<sup>†</sup>  $^{63}\text{Cu}$  NMR relaxation rate measurements were used to determine the equilibrium bath temperature  $T = 25$  mK. As in our previous work (13), low-power RF experiments were carried out to make sure the results were not measurably altered by RF pulse heating effects. The applied field strength  $B$  was determined to within uncertainties less than tens of  $\mu\text{T}$  from the NMR resonance of  $^3\text{He}$  in the  $^3\text{He}/^4\text{He}$  mixture of the dilution refrigerator.

**Data Availability.** Excel data have been deposited in <https://www.pa.ucla.edu/content/sr2ruo4-knightshift-vs-field/>.

**ACKNOWLEDGMENTS.** We thank Thomas Scaffidi and Steve Kivelson for a number of helpful discussions. A.C. is grateful for support from the Julian Schwinger Foundation for Physics Research. A.P. acknowledges support by the Alexander von Humboldt Foundation through the Feodor Lynen Fellowship. Work at Los Alamos was funded by Laboratory Directed Research and Development (LDRD) program, and A.P. acknowledges partial support through the LDRD. N.K. acknowledges the support by the Grants-in-Aid for Scientific Research (KAKENHI, Grant JP18K04715 and JP21H01033) from Japan Society for the Promotion of Science (JSPS). The work at Dresden was funded by the Deutsche Forschungsgemeinschaft - TRR 288 - 422213477 (projects A10 and B01). The work at University of California, Los Angeles, was supported by NSF Grants 1709304 and 2004553.

1. A. P. Mackenzie, T. Scaffidi, C. W. Hicks, Y. Maeno, Even odder after twenty-three years: The superconducting order parameter puzzle of  $\text{Sr}_2\text{RuO}_4$ . *npj Quant. Mater.* **2**, 40 (2017).
2. C. Kallin, Chiral  $p$ -wave order in  $\text{Sr}_2\text{RuO}_4$ . *Rep. Prog. Phys.* **75**, 042501 (2012).
3. A. P. Mackenzie, Y. Maeno, The superconductivity of  $\text{Sr}_2\text{RuO}_4$  and the physics of spin-triplet pairing. *Rev. Mod. Phys.* **75**, 657–712 (2003).
4. Y. Maeno *et al.*, Superconductivity in a layered perovskite without copper. *Nature* **372**, 532–534 (1994).
5. T. M. Rice, M. Sigrist,  $\text{Sr}_2\text{RuO}_4$ : An electronic analogue of  $^3\text{He}$ ? *J. Phys. Condens. Matter* **7**, L643–L648 (1995).
6. K. Ishida *et al.*, Spin-triplet superconductivity in  $\text{Sr}_2\text{RuO}_4$  identified by  $^{17}\text{O}$  Knight shift. *Nature* **396**, 658–660 (1998).
7. G. M. Luke *et al.*, Time-reversal symmetry-breaking superconductivity in  $\text{Sr}_2\text{RuO}_4$ . *Nature* **394**, 558 (1998).
8. J. Xia, Y. Maeno, P. T. Beyersdorf, M. M. Fejer, A. Kapitulnik, High resolution Polar Kerr Effect measurements of  $\text{Sr}_2\text{RuO}_4$ : Evidence for broken time-reversal symmetry in the superconducting state. *Phys. Rev. Lett.* **97**, 167002 (2006).
9. E. Hassinger *et al.*, Vertical line nodes in the superconducting gap structure of  $\text{Sr}_2\text{RuO}_4$ . *Phys. Rev. X* **7**, 011032 (2017).
10. S. Kittaka *et al.*, Searching for gap zeros in  $\text{Sr}_2\text{RuO}_4$  via field-angle-dependent specific-heat measurement. *J. Phys. Soc. Jpn.* **87**, 093703 (2018).
11. S. Yonezawa, T. Kajikawa, Y. Maeno, First-order superconducting transition in  $\text{Sr}_2\text{RuO}_4$ . *Phys. Rev. Lett.* **110**, 077003 (2013).
12. S. Yonezawa, T. Kajikawa, Y. Maeno, Specific-heat evidence of the first-order superconducting transition in  $\text{Sr}_2\text{RuO}_4$ . *J. Phys. Soc. Jpn.* **83**, 083706 (2014).
13. A. Pustogow *et al.*, Constraints on the superconducting order parameter in  $\text{Sr}_2\text{RuO}_4$  from oxygen-17 nuclear magnetic resonance. *Nature* **574**, 72–75 (2019).
14. K. Ishida, M. Manago, K. Kinjo, Y. Maeno, Reduction of the  $^{17}\text{O}$  Knight Shift in the superconducting state and the heat-up effect by NMR pulses on  $\text{Sr}_2\text{RuO}_4$ . *J. Phys. Soc. Jpn.* **89**, 34712 (2020).
15. A. T. Römer, D. D. Scherer, I. M. Eremin, P. J. Hirschfeld, B. M. Andersen, Knight shift and leading superconducting instability from spin fluctuations in  $\text{Sr}_2\text{RuO}_4$ . *Phys. Rev. Lett.* **123**, 247001 (2019).
16. H. S. Röising, T. Scaffidi, F. Flicker, G. F. Lange, S. H. Simon, Superconducting order of  $\text{Sr}_2\text{RuO}_4$  from a three-dimensional microscopic model. *Phys. Rev. Res.* **1**, 033108 (2019).
17. B. Keimer, S. A. Kivelson, M. R. Norman, S. Uchida, J. Zaanen, From quantum matter to high-temperature superconductivity in copper oxides. *Nature* **518**, 179–186 (2015).
18. J. Mravlje *et al.*, Coherence-incoherence crossover and the mass-renormalization puzzles in  $\text{Sr}_2\text{RuO}_4$ . *Phys. Rev. Lett.* **106**, 96401 (2011).
19. A. Damascelli *et al.*, Fermi surface, surface states, and surface reconstruction in  $\text{Sr}_2\text{RuO}_4$ . *Phys. Rev. Lett.* **85**, 5194–5197 (2000).

20. A. Tamai *et al.*, High-resolution photoemission on  $\text{Sr}_2\text{RuO}_4$  reveals correlation-enhanced effective spin-orbit coupling and dominantly local self-energies. *Phys. Rev. X* **9**, 021048 (2019).
21. S. A. Kivelson, A. C. Yuan, B. Ramshaw, R. Thomale, A proposal for reconciling diverse experiments on the superconducting state in  $\text{Sr}_2\text{RuO}_4$ . *npj Quant. Mater.* **5**, 43 (2020).
22. A. Steppke *et al.*, Strong peak in  $T_c$  of  $\text{Sr}_2\text{RuO}_4$  under uniaxial pressure. *Science* **355**, eaaf9398 (2017).
23. Y. Amano, M. Ishihara, M. Ichioka, N. Nakai, K. Machida, Pauli paramagnetic effects on mixed-state properties in a strongly anisotropic superconductor: Application to  $\text{Sr}_2\text{RuO}_4$ . *Phys. Rev. B* **91**, 144513 (2015).
24. S. NishiZaki, Y. Maeno, Z. Mao, Changes in the superconducting state of  $\text{Sr}_2\text{RuO}_4$  under magnetic fields probed by specific heat. *J. Phys. Soc. Jpn.* **69**, 572–578 (2000).
25. T. Imai, A. W. Hunt, K. R. Thurber, F. C. Chou,  $^{17}\text{O}$  NMR evidence for orbital dependent ferromagnetic correlations in  $\text{Sr}_2\text{RuO}_4$ . *Phys. Rev. Lett.* **81**, 3006–3009 (1998).
26. Y. Luo *et al.*, Normal state  $^{17}\text{O}$  NMR studies of  $\text{Sr}_2\text{RuO}_4$  under uniaxial stress. *Phys. Rev. X* **9**, 021044 (2019).
27. H. Murakawa *et al.*,  $^{101}\text{Ru}$  Knight Shift measurement of superconducting  $\text{Sr}_2\text{RuO}_4$  under small magnetic fields parallel to the  $\text{RuO}_2$  plane. *J. Phys. Soc. Jpn.* **76**, 024716 (2007).
28. G. E. Volovik, Superconductivity with lines of gap nodes - density-of-states in the vortex. *JETP Lett.* **58**, 469–473 (1993).
29. C. N. Veenstra *et al.*, Spin-orbital entanglement and the breakdown of singlets and triplets in  $\text{Sr}_2\text{RuO}_4$  revealed by spin- and angle-resolved photoemission spectroscopy. *Phys. Rev. Lett.* **112**, 127002 (2014).
30. S. Mazumdar, Negative charge-transfer gap and even parity superconductivity in  $\text{Sr}_2\text{RuO}_4$ . *Phys. Rev. Res.* **2**, 023382 (2020).
31. R. Sharma *et al.*, Momentum-resolved superconducting energy gaps of  $\text{Sr}_2\text{RuO}_4$  from quasiparticle interference imaging. *Proc. Natl. Acad. Sci. U.S.A.* **117**, 5222–5227 (2020).
32. C. M. Puetter, H.-Y. Kee, Identifying spin-triplet pairing in spin-orbit coupled multi-band superconductors. *Europhys. Lett.* **98**, 27010 (2012).
33. H. G. Suh *et al.*, Stabilizing even-parity chiral superconductivity in  $\text{Sr}_2\text{RuO}_4$ . *Phys. Rev. Res.* **2**, 032023 (2020).
34. A. W. Lindquist, H.-Y. Kee, Distinct reduction of knight shift in superconducting state of  $\text{Sr}_2\text{RuO}_4$  under uniaxial strain. *Phys. Rev. Res.* **2**, 032055 (2020).
35. T. Scaffidi, Degeneracy between even- and odd-parity superconductivity in the quasi-1d hubbard model and implications for  $\text{Sr}_2\text{RuO}_4$ . arXiv [Preprint] (2020). <https://arxiv.org/abs/2007.13769> (Accessed 28 April 2021).
36. S. Ghosh *et al.*, Thermodynamic evidence for a two-component superconducting Order Parameter in  $\text{Sr}_2\text{RuO}_4$ . *Nat. Phys.* **17**, 199–204 (2021).
37. S. Benhabib *et al.*, Ultrasound evidence for a two-component superconducting order parameter in  $\text{Sr}_2\text{RuO}_4$ . *Nat. Phys.* **17**, 194–198 (2021).
38. R. Willa, M. Hecker, R. M. Fernandes, J. Schmalian, Inhomogeneous time-reversal symmetry breaking in  $\text{Sr}_2\text{RuO}_4$ . arXiv [Preprint] (2020). <https://arxiv.org/abs/2011.01941> (Accessed 28 April 2021).
39. A. T. Römer, P. J. Hirschfeld, B. M. Andersen, Superconducting state of  $\text{Sr}_2\text{RuO}_4$  in the presence of longer-range coulomb interactions. arXiv [Preprint] (2021). <https://arxiv.org/abs/2101.06972> (Accessed 28 April 2021).
40. V. Grinenko *et al.*, Split superconducting and time-reversal symmetry-breaking transitions in  $\text{Sr}_2\text{RuO}_4$  under stress. *Nat. Phys.* **17**, 748–754 (2021).
41. R. K. Harris, E. D. Becker, S. M. Cabral de Menezes, R. Goodfellow, P. Granger, NMR nomenclature, nuclear spin properties and conventions for chemical shifts (IUPAC recommendations 2001). *Pure Appl. Chem.* **73**, 1795–1818 (2001).